UDC 620.9
DOI: 10.53297/18293328-2024.2-102

# TECHNO-ECONOMIC ANALYSIS OF AN OFF-GRID SOLAR POWER PLANT INTEGRATED WITH A HYDROGEN STORAGE SYSTEM: A CASE STUDY OF HANKAVAN, ARMENIA

**R.H. Avoyan**

*National Polytechnic University Of Armenia*

A solar photovoltaic (PV) power plant integrated with a hydrogen storage system (PV-$H_2$-SS) is proposed as an off-grid power supply solution for a case study site in Hankavan, Armenia. The load profile and available energy resources for the chosen site is generated, and based on this, the major system components – namely, the PV system, electrolyzer, fuel cell, Li-ion battery, hydrogen storage, and compressor – are sized accordingly. The operational performance of a solar PV-$H_2$-SS system is analyzed to ensure a reliable electricity supply throughout the year. The operational analysis results confirm that all components are selected in accordance with the required capacity and are aligned with the energy needs. Hydrogen is primarily produced during the summer for winter energy supply and is used to cover the daytime (06:00–00:00) energy deficit, while the PV system generates sufficient electricity each day to charge the Li-ion battery. The battery serves as a short-term energy buffer, covering the daytime energy deficit for 5 minutes to allow the fuel cell to warm up and supplying the standby load at night (00:00-06:00). By integrating Li-ion batteries for short-term use and hydrogen storage for long-term use, the system efficiently balances energy resources throughout the year. To evaluate the feasibility of the off-grid PV-$H_2$-SS, the levelized cost of electricity (LCOE) is compared with that of an electrical grid extension. The break-even distance for the case study site is determined to be 3 *km*. The calculated LCOE for the solar PV-$H_2$-SS is 1.48 *$/kWh*, whereas the LCOE for a grid extension of 3 *km* is 1.51 *$/kWh*. Based on these findings, the off-grid PV-$H_2$-SS is considered economically feasible for installation at the case study site if it is located 3 *km* or more from the grid, providing a clean and sustainable alternative for decentralized off-grid electrification. Additionally, the obtained results indicate that the PV-$H_2$-SS can be scaled or adapted for use in rural areas remote from centralized energy networks, where constructing new infrastructure would require substantial investment.

***Keywords:*** solar photovoltaic system, hydrogen storage system, electrolyzer, fuel cell, Li-ion battery, compressor, levelized cost of electricity.

***Introduction.*** Global energy demand has been steadily increasing, leading to record-high carbon dioxide ($CO_2$) emissions in recent years. In 2023, energy-related $CO_2$ emissions reached approximately 37.4 billion tonnes, marking a new historical peak. This trend underscores the urgent need for cleaner and more sustainable energy sources. Solar photovoltaic (PV) technology has emerged as a key component of the global transition to renewable energy due to its rapid expansion and lack of

operational emissions. In 2023, global solar PV installations reached unprecedented levels, adding hundreds of gigawatts of new capacity. This widespread deployment is crucial for mitigating $CO_2$ emissions and sustainably meeting rising global energy demands [1].

Despite these advancements, a significant portion of the global population particularly in remote and rural areas still lacks access to electricity. Off-grid solar PV systems offer a promising solution for electrification in these regions, where extending the centralized grid is often technically challenging or economically unfeasible [2].

However, solar energy is inherently intermittent, with no generation at night and reduced output on cloudy days, necessitating energy storage solutions for off-grid systems. Lithium-ion (Li-ion) batteries are the most common storage technology, offering high efficiency and fast response times for energy supply [3]. However, they have limitations in long-term or seasonal storage due to their self-discharge losses and cycle life constraints. Maintaining large battery banks to cover seasonal deficits can also be cost-prohibitive and susceptible to performance degradation in extreme temperatures [4]. These drawbacks highlight the need for complementary storage solutions capable of managing longer storage durations beyond what batteries alone can provide.

Hydrogen is gaining recognition as a viable medium for long-term and seasonal energy storage in solar power systems. Surplus solar power can be used for electrolysis to produce hydrogen, which can be stored for days, months, or even seasons. Unlike batteries, hydrogen storage does not experience significant self-discharge and can be scaled for large energy capacities [5,6]. However, hydrogen fuel cells require several seconds or even minute to reach full power output [7,8]. To address this limitation, hybrid systems integrating hydrogen storage with Li-ion batteries have been proposed, leveraging the strengths of both technologies. This approach enables a near-100% renewable energy supply for remote off-grid applications.

This study aims to assess the technical and economic performance of an off-grid solar PV power plant integrated with a hydrogen storage system (PV-$H_2$-SS). This research focuses on a case study in Armenia, where no previous studies have explored the feasibility of such a system for off-grid use. By analyzing primary field data, this study provides essential insights into the integration of solar PV with hydrogen storage in Armenia. It serves as a foundation for future research in this area.

***Methodology***. In this study, a four-student apartment has been selected as the research subject. The apartment is part of the Polytechnic Educational and Wellness Camp located in Hankavan, Armenia. It is equipped with all the necessary electrical appliances, which are described in detail below.

Given the practical implementation of such energy projects in real-world conditions, it is advisable to initially deploy advanced technologies in public buildings. This approach allows for a comprehensive evaluation of their efficiency and feasibility. Based on the obtained results, the system can be scaled or adapted for use in areas that are remote from centralized energy networks, where constructing new infrastructure would require substantial investment.

This study employs a descriptive methodology, which includes:

- Analysis of energy demand and available resources.
- System sizing, considering energy generation, storage, and consumption.
- Techno-economic assessment to determine the feasibility of the proposed solutions.

The subsequent sections outline the step-by-step methodology employed in this study.

***Analysis of demand and resources.*** The load profile is generated based on the operation of electrical appliances in the apartment and is developed following the methodology described in [9,10]. It incorporates key parameters such as the number of electrical appliances used, their operating time, nominal power, and the coincidence factor. The electrical appliances utilized in the apartment, along with their nominal power ratings, are presented in *Table 1*.

*Table 1*

*List of electrical appliances with their nominal power and quantity*

| № | Electrical appliances | Nominal power (Watt) | Quantity |
|---|---|---|---|
| 1 | Lamps | 30 | 10 |
| 2 | Exterior Lamps | 60 | 3 |
| 3 | TV | 150 | 1 |
| 4 | Wi-Fi router | 50 | 1 |
| 5 | Laptop | 150 | 4 |
| 6 | Phone charger | 30 | 4 |
| 7 | Washing machine | 600 | 1 |
| 8 | Vacuum cleaner | 300 | 1 |
| 9 | Refrigerator | 400 | 1 |
| 10 | Electric oven | 2000 | 1 |

These initial data were collected through direct observation at the study site. The operating hours for all electrical appliances are from 06:00 to 00:00, except for refrigerators and the Wi-Fi router, which operate continuously, as well as outdoor lighting, which is activated only at night from 20:00 to 06:00.

Although all electrical appliances are installed, they are not used simultaneously throughout the day. Their operating time varies, so a coincidence

factor is applied to estimate the daily energy consumption and peak load. This factor (ranging from 0 to 1) reflects the probability of multiple appliances operating at full capacity simultaneously. For this facility, the coincidence factor was determined through observational analysis of appliance usage. The corresponding values are presented in *Table 2*.

*Table 2*

*The hourly coincidence factor (data obtained through direct observation)*

| Time | Coincidence factor | Time | Coincidence factor | Time | Coincidence factor |
|---|---|---|---|---|---|
| 00:00-01:00 | 0,134 | 08:00-09:00 | 0,217 | 16:00-17:00 | 0,255 |
| 01:00-02:00 | 0,134 | 09:00-10:00 | 0,28 | 17:00-18:00 | 0,383 |
| 02:00-03:00 | 0,134 | 10:00-11:00 | 0,255 | 18:00-19:00 | 0,553 |
| 03:00-04:00 | 0,134 | 11:00-12:00 | 0,255 | 19:00-20:00 | 0,553 |
| 04:00-05:00 | 0,134 | 12:00-13:00 | 0,255 | 20:00-21:00 | 0,383 |
| 05:00-06:00 | 0,134 | 13:00-14:00 | 0,255 | 21:00-22:00 | 0,383 |
| 06:00-07:00 | 0,153 | 14:00-15:00 | 0,255 | 22:00-23:00 | 0,229 |
| 07:00-08:00 | 0,153 | 15:00-16:00 | 0,255 | 23:00-00:00 | 0,229 |

The load profile, based on the values of the coincidence factor, is defined by the following equation:

$$P_h = CF_h \sum_i^{Appliance} P_i \times \sum_1^j Q_j, \quad (1)$$

where $P_h$ is the power demand at hour $h$ ($kW$); $P_i$ - the nominal power of appliance $i$ ($kW$); $CF_h$ - the coincidence factor at hour $h$ and $Q_j$ - the quantity of appliances used. This equation determines the power required for the apartment for each hour of the day.

For the electric load and corresponding quantity data presented in *Table 1*, along with the coincidence factors listed in *Table 2*, the load profile for the selected building is generated by applying *Eq. (1)*, as illustrated in *Fig. 1*.

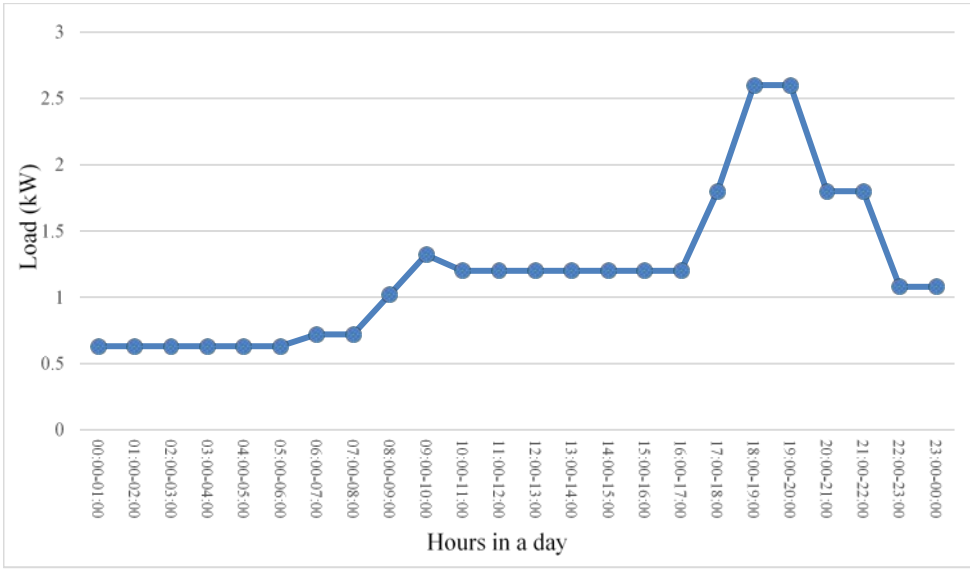


*Fig. 1. Hourly load profile of the case study site*

From the analysis in *Fig. 1*, the peak load of the case study site is 2.6 *kW*, while the nighttime standby load is 0.63 *kW*. The total daily electricity consumption is 28.72 *kWh*.

Since the case study site does not utilize electricity for heating or cooling, the presented load profile remains consistent throughout the year. By integrating $P_h$ from *Eq. (1)* with the usage hours, the annual electricity demand is found to be 10482.8 *kWh*.

Considering the presence of PV panels in the system, an analysis of solar radiation data for the case study site was conducted. Hourly values of global horizontal irradiation at a tilt angle of 22° were obtained using the PVGIS tool. The results of the analysis are presented in *Fig. 2*. The annual irradiation at the case study site was found to be approximately 1422 *kWh/m²*.

***System sizing.*** Once the demand and available resources have been assessed, the sizing of the off-grid solar PV-$H_2$-SS is determined. It is designed for installation at the case study site and was developed in [11]. Its main components include PV panels, an inverter, a Li-ion battery, an electrolyzer, a compressor, a high-pressure hydrogen storage tank, and a fuel cell.

The PV sizing follows the methodology outlined in [12], ensuring that the annual PV generation aligns with the annual load demand. The calculation is conducted following the given equation:

$$P_{PV} = \frac{E_d \times I_{STC}}{I_{GHI} \times PR \times \eta_{el} \times \eta_{fc}}, \quad (2)$$

where $P_{PV}$ is the required installed capacity of solar PV panels (*kW*); $E_d$ - the annual electricity demand in *kWh*; $I_{STC}$ - the solar irradiation under standard test conditions (STC, 1 *kW/m²*); $I_{GHI}$ - the annual global horizontal irradiation on an inclined surface (*kWh/m²*), the performance ratio (*PR*) of the solar PV system, typically taken as 0.9, represents the overall system efficiency, accounting for losses due to shading, dust accumulation, and balance of the system (BOS) components, including inverters, cables, connections, and batteries. Furthermore, $\eta_{el.}$ denotes the electrolyzer efficiency, which for a proton exchange membrane (PEM) electrolyzer is typically around 80% [13], while $\eta_{fc.}$ represents the fuel cell efficiency, which for a PEM fuel cell is typically around 50% [14].

Thus, based on the annual energy demand and the annual global horizontal irradiation on an inclined surface, as determined in the previous section, and by applying *Eq. (2)*, the required installed capacity of the PV panels was calculated to be 20.47 *kW*. Considering a weighted approach, PV solar panels with a total capacity of 25 *kW* were selected for this study (The inverter capacity is equal to the total capacity of the PV panels).

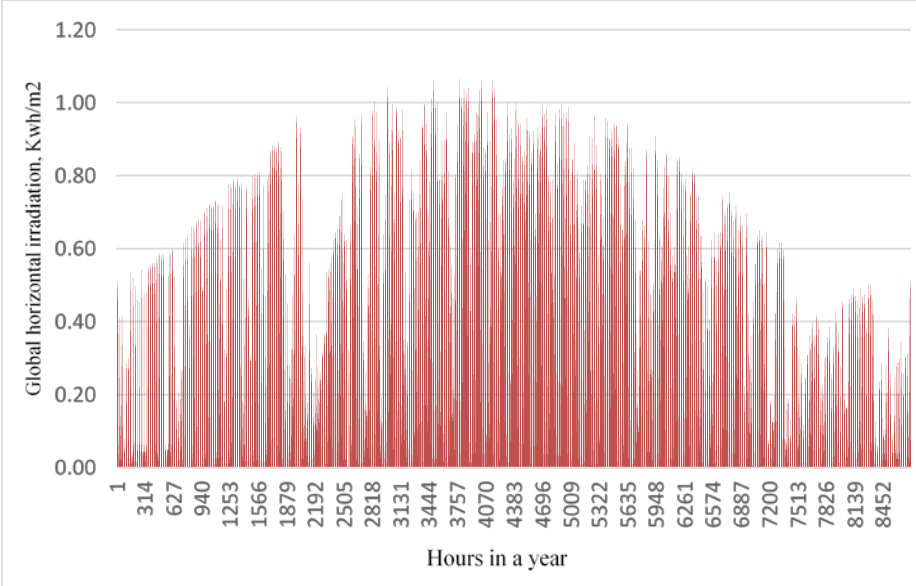


*Fig. 2. The hourly solar radiation in Hankavan, Armenia*

Subsequently, the selected capacity of the PV solar panels is analyzed on an hourly basis to assess the surplus and deficit, evaluating their ability to meet the required electrical load at each hour.

The hourly energy generation corresponding to the selected nominal capacity of the solar PV panels ($P_{PV}$) is calculated using *Eq.(3)*:

$$E_{PVh} = \frac{P_{PV} \times I_{GHIh} \times PR}{I_{STC}}, \quad (3)$$

where $E_{PVh}$ represents the electricity generation from the PV panels at hour $h$.

The hourly surplus or deficit ($E_{net}$) is determined based on the balance between generated and consumed energy and is calculated using the corresponding equation:

$$E_{net} = E_{PVh} - P_h \times h, \quad (4)$$

where $h$ denotes the duration of the $P_h$ load.

Thus, by calculating the hourly electricity generation from PV panels over the course of a year and incorporating the hourly electrical load profile, the hourly energy balance is determined using *Eq. (4)*, facilitating the identification of surplus or deficit for each hour. The obtained results are presented in *Fig. 3.*

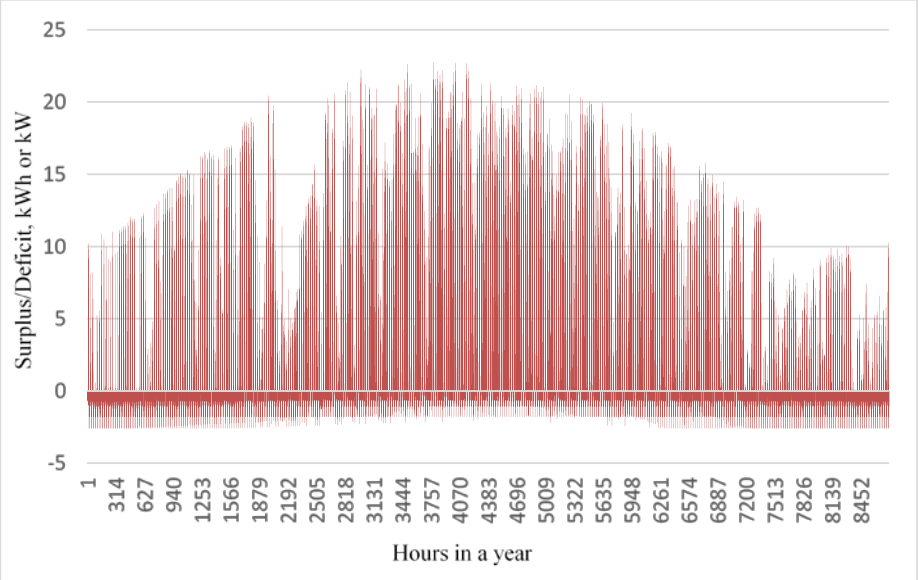


*Fig. 3. The hourly surplus/deficit analysis for the selected PV size (25 kW)*

From the analysis in *Fig.3*, the observed deficit values are primarily due to the unavailability of solar radiation, such as during nighttime or cloudy days. Additionally, peak surplus values exceeding 22 *kW* are observed, predominantly occurring when the system generates electricity under the conditions of minimal demand and high solar radiation, particularly in the summer.

In this off-grid PV-$H_2$-SS, according to [11], a Li-ion battery functions as short-term storage, providing energy for nighttime standby loads (00:00–06:00) and covering the daytime deficits (06:00–00:00) for five minutes to allow the fuel cell to reach an operational state. The battery must have sufficient capacity to meet nighttime standby loads as well as the worst-case daytime energy demands.

To achieve a more accurate and detailed analysis, battery sizing is performed using the maximum cumulative deficit method rather than the autonomy days approach. The autonomy days method typically leads to an oversized battery capacity. The calculation is conducted following the given equation:

$$E_{bat} = \frac{E_{cumul.max}}{(SoC_{max} - SoC_{min}) \times \eta_{Bat}}, \quad (5)$$

where $E_{bat}$ represents the required battery capacity (kWh), $E_{cumul.max}$ denotes the maximum cumulative deficit, which, in this case, corresponds to the maximum daily deficit that the battery needs to cover. The maximum state of charge of the Li-ion battery ($SoC_{max}$) is assumed to be 85%, while the minimum state of charge ($SoC_{min}$) is assumed to be 20%. Additionally, $\eta_{bat}$ represents the efficiency of the Li-ion battery system, which is assumed to be 95% [15].

The cumulative deficit is calculated by summing the nighttime hourly deficits (00:00–06:00) and the daytime 5-minute deficits (06:00–00:00) from *Fig.3*. At the beginning of each new day, the cumulative deficit is reset to zero. This process is repeated for all 8,760 hours of the analysis period. The obtained results are presented in *Fig. 4*.

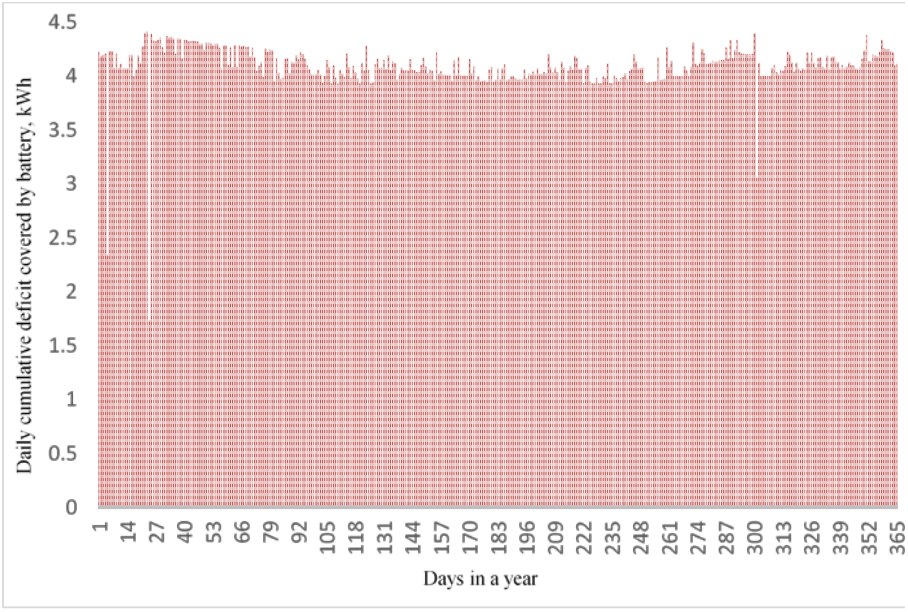


*Fig. 4. The daily cumulative deficit that the battery must supply*

From the analysis in *Fig.4*, the maximum daily energy deficit (i.e., the maximum cumulative deficit) that the battery must cover is determined to be 4.41 *kWh*. Based on this value, taking into account the maximum and minimum state of charge (*SoC*), the battery efficiency, and using *Eq. (5)*, the required battery storage

capacity is calculated to be 7.14 *kWh*. To ensure a reliable approach, a Li-ion battery with a capacity of 10 *kWh* is selected for this case study site.

In this solar PV-$H_2$-SS, the fuel cell must generate sufficient power to compensate for the energy deficit, even under the most extreme weather conditions when no electricity is produced by the PV panels. Following this approach, the nominal power of the fuel cell is determined based on the peak deficit load observed throughout the year, ensuring a reliable and uninterrupted power supply. According to this principle, the rated nominal power of the fuel cell can be calculated using the following expression:

$$P_{FC} = P_{def,max},$$

where $P_{def,max}$ represents the maximum daytime deficit power over the course of 8,760 hours.

To determine the maximum deficit power that the fuel cell must supply, the deficit values from *Fig. 3* were analyzed for the daytime period (06:00–00:00). This analysis considers the battery's compensation for the deficit during the first five minutes. The results are presented in *Fig.5*.

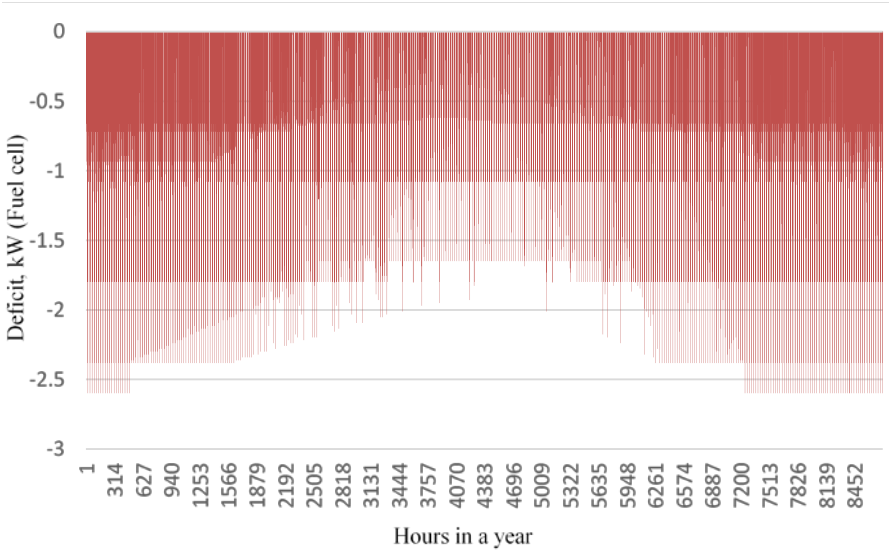


*Fig.5. The hourly deficit power that the fuel cell must cover*

Based on the analysis presented in *Fig. 5*, the maximum power deficit was determined to be 2.6 *kW*. Considering a weighted approach, a PEM fuel cell with a capacity of 3 *kW* was selected for this case study site. The PEM fuel cell has a specific hydrogen consumption rate of 0.8 $Nm^3$ per *kWh* of electricity produced and a system efficiency of 50% [14,16].

In this solar PV-$H_2$-SS, the electrolyzer operates during solar hours when surplus electricity is available, and the Li-ion battery reaches its maximum SoC [11]. According to this methodology, the nominal power of the electrolyzer is defined as the peak surplus power observed throughout the year when the Li -ion battery's SoC reaches 85%. This can be presented by the following equation:

$$P_{el} = \max(P_{sur}) \,|SoC = 85\%,$$

where $P_{el}$ represents the nominal power of the electrolyzer ($kW$); $P_{sur}$ denotes the surplus electrical power available in the system ($kW$), and $SoC$ refers to the state of charge of the Li-ion battery. The equation determines the maximum surplus power observed throughout the year when the Li-ion battery's SoC is at 85%.

To identify the maximum surplus power at which the electrolyzer operates, the surplus values from *Fig.3* were analyzed, assuming the battery is fully charged. The resulting data are presented in *Fig.6*.

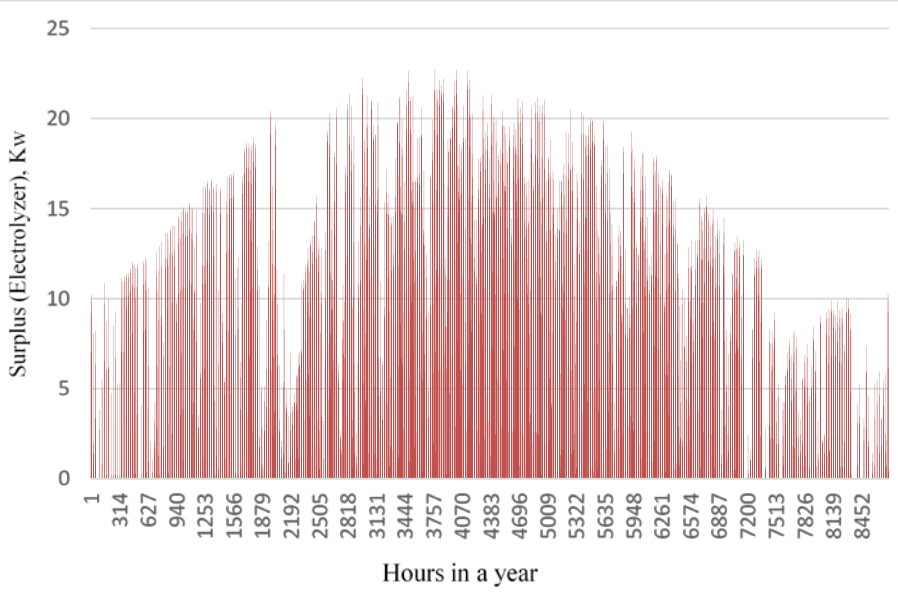


*Fig. 6. The hourly surplus power for electrolyzer*

According to the analysis presented in *Fig.6*, the maximum surplus power of 22.74 *kW* is observed at the 3,782nd hour of the year. Based on this analysis, a PEM electrolyzer with a capacity of 23 *kW* was selected for this case study site. The electrolyzer has a hydrogen production rate of 5 *kWh/Nm³* at an output pressure of 30 bar [13].

Hydrogen storage is utilized to store the hydrogen produced by the electrolyzer and compressed by the compressor. To determine the appropriate size

of the hydrogen storage tank, it is first necessary to analyze the hydrogen production and consumption over time. Since the selected PEM electrolyzer produces 1 *Nm³* of hydrogen by consuming 5 *kWh* of electricity, the hourly hydrogen production can be calculated by multiplying each surplus energy value from *Fig.6* by 0.2. Similarly, as the selected PEM fuel cell generates 1 *kWh* of electricity by consuming 0.8 *Nm³* of hydrogen, the hourly hydrogen consumption can be determined by multiplying each deficit energy value from *Fig.5* by 0.8. The results obtained are presented in *Fig.7.*

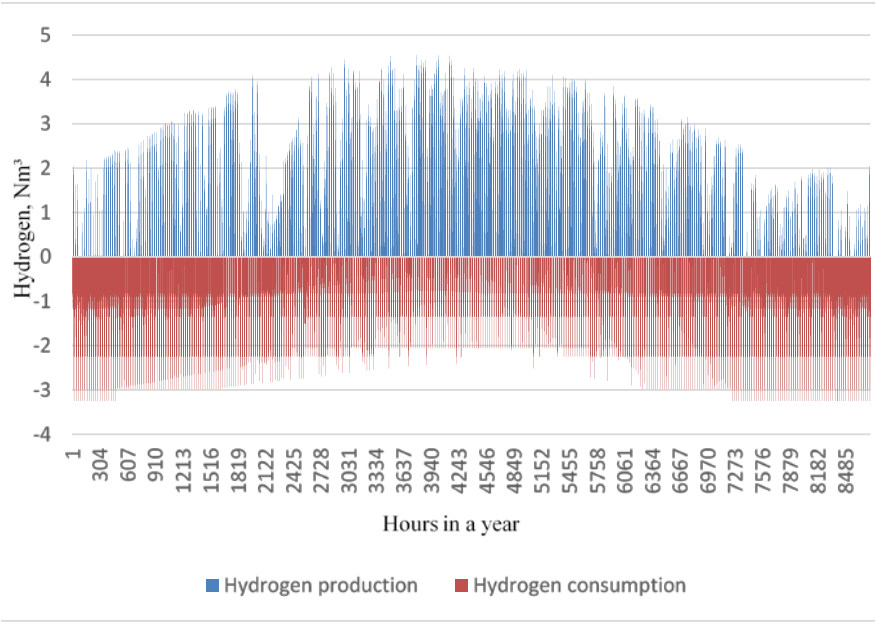


*Fig. 7. The hourly production and consumption of hydrogen*

According to the analysis in *Fig.7*, hydrogen production peaks from mid-spring to late summer when consumption remains relatively low. In contrast, during winter, hydrogen consumption exceeds production. To ensure efficient operation, the off-grid PV-H2-SS should not start in winter when PV electricity generation is lower than demand. An off-grid system should ideally commence operation when daily energy generation exceeds consumption. Based on this criterion, the system is assumed to begin operation at 2,604 hours, corresponding to April 19th at noon.

To determine the optimal size of the hydrogen storage tank, it is essential to calculate the maximum amount of hydrogen that can be stored at any given time. This is achieved by evaluating the cumulative hydrogen production over the operating period. The stored hydrogen mass at hour *h* (starting from hour 1 of operation, which corresponds to April 19th at noon, and continuing until the 8760th hour) can be calculated as follows:

$$m_{H2}(h) = \int_1^h \left[\dot{m}_{H2,prod}(h') - \dot{m}_{H2,cons}(h')\right] dh', \quad (6)$$

where $\dot{m}_{H2,prod}(t')$ is the rate of hydrogen production (mass flow rate of hydrogen generation, *kg/h*) at time $t'$ and $\dot{m}_{H2,cons}(h')$ is the rate of hydrogen consumption (mass flow rate of hydrogen usage, *kg/h*) at time $t'$.

The maximum cumulative hydrogen for storage over the entire year is determined by:

$$m_{H2,max} = \max_{h\in[1,8760]} \{m_{H2}(h)\}.$$

To convert this maximum mass of hydrogen into the required tank volume, the Van der Waals equation is applied [17]:

$$P_{tank} = \frac{m_{H2,max}}{M_{H2}} \times \frac{R\times T}{V_{tank}-nb} \times a \times \frac{1}{V_{tank}^2} \times \left(\frac{m_{H2,max}}{M_{H2}}\right)^2, \quad (7)$$

where R is the universal gas constant (8.314 *J/mol·K*); T - the absolute operating temperature (assumed to be 298.15 *K*, corresponding to a storage temperature of 25 °C); $M_{H2}$ - the molar mass of hydrogen (0.002016 *kg/mol*), and $P_{tank}$ - the storage pressure (assumed to be 350 bar, equivalent to $35\times10^6$ *Pa*); $V_{tank}$ - required tank volume; *a* - the dipole interaction or repulsion constant ($a=2.476\times10^{-2}$ $m^3\cdot Pa\cdot mol^{-2}$) and *b* - the volume occupied by the hydrogen molecules ($b=2.661\times10^{-5}$ $m^3\cdot mol^{-1}$).

Accordingly, by applying *Eq.(6)* to each hour in *Fig.7*, the cumulative hydrogen production for every hour is determined. The maximum cumulative hydrogen is found to be 1,958 *Nm³*, which corresponds to $m_{H2,max}$ = 176 *kg*. Using this value in *Eq.(7)* and solving for $V_{tank}$ numerically, the required hydrogen tank size at a storage pressure of 350 bar is calculated to be 8 *m³*.

Hydrogen has a low volumetric energy density in both its gaseous and liquid states due to its low atomic mass, despite having a high gravimetric energy density. To improve its storage viability, its volumetric energy density must be increased. One common method is compression, which reduces the hydrogen volume by increasing its pressure. A hydrogen compressor is a device that elevates hydrogen pressure, thereby minimizing its storage volume. In the proposed PV-H2-SS, hydrogen generated by the electrolyzer is directed to a compressor before being stored in a designated hydrogen storage tank. The power required for hydrogen compression is determined using the following equation [18]:

$$P_{comp} = \frac{1}{\eta_{comp}} \times \frac{k}{(k-1)} \times \dot{m}_{H2,max} \times \frac{R\times T}{M_{H2}} \times \left(\left(\frac{p_2}{p_1}\right)^{\frac{k-1}{k}} - 1\right), \quad (8)$$

where $\eta_{comp}$ (taken 0.7) represents the compressor efficiency; $\dot{m}_{H2,max}$ (*kg/s*) denotes the maximum mass flow rate of hydrogen entering the compressor, and k represents the heat capacity ratio (1.41 for hydrogen). The pressures before and after

compression are denoted as $p_1$ (for the selected electrolyzer, 30 bar = $30\times10^5$ *Pa*) and $p_2$ (for the chosen hydrogen storage tank, 350 bar = $35\times10^6$ *Pa*), respectively.

According to the analysis presented in *Fig. 7*, the maximum mass flow rate of hydrogen produced by the electrolyzer is 4.548 $Nm^3/h$, which corresponds to 0.4 *kg/h*. For secondary production, the mass flow rate would be $1.1\times10^{-4}$ *kg/s*. Using this value in *Eq.(8)*, the power capicity for compressor found to be 0,676 *kW*. Considering a conservative approach, the compressor with a capacity of 0,7 *kW* is chosen for this case study site.

***Techno-economic assessment.*** After finalizing the sizing of the off-grid solar PV-$H_2$-SS, it is crucial to assess its overall performance. From a technical standpoint, validating the PV-$H_2$-SS is necessary to ensure that the selected capacity aligns with the energy needs. On the economic side, components related to hydrogen, such as electrolyzers, compressors, storage units, and fuel cells, involve significant costs. Therefore, conducting a financial evaluation is essential to determine whether the PV-$H_2$-SS is economically viable.

Based on the load profile, available energy resources, and PV-$H_2$-SS sizing, and considering the proposed energy management algorithm in [11], a one-year operational performance analysis of an off-grid PV-$H_2$-SS at the Polytechnic Educational and Wellness Camp has been conducted.

The total energy demand over the year is $10.4828\times10^3$ *kWh*, while the PV generation for the same period is $31.999\times10^3$ *kWh*, which is approximately three times higher than the load demand. This excess PV generation is necessary to account for the low efficiencies of the electrolyzer, which converts surplus PV energy into hydrogen, and the fuel cell, which generates electricity from the stored hydrogen.

The electrolyzer produces 5,111 $Nm^3$ (459 *kg*) of hydrogen over the course of the year, while the fuel cell consumes 5,053 $Nm^3$ (455 *kg*) of hydrogen annually to compensate for the energy deficit.

The energy state of the hydrogen storage tank throughout the year is summarized in *Fig. 8*. At the beginning of operation, surplus PV generation is utilized to produce hydrogen via the electrolyzer. During the summer months, hydrogen storage gradually increases until it reaches its maximum capacity of 176 *kg*. Toward the end of the year and the beginning of the next (during winter), hydrogen storage declines as it is consumed by the fuel cell to generate electricity and meet the load demand. From *Fig.8*, it is evident that there is always a sufficient amount of hydrogen available to cover energy deficits.

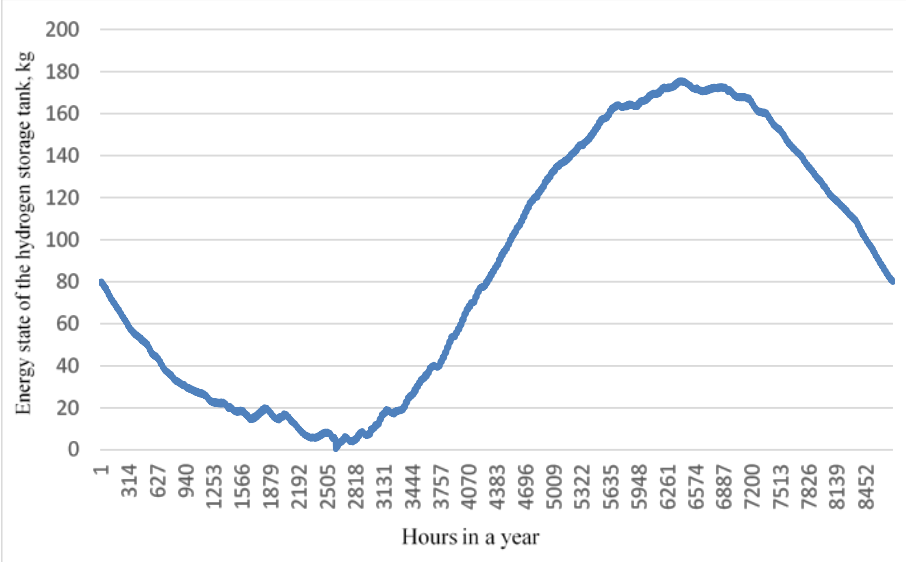


*Fig. 8. The energy state of hydrogen storage tank (kg) throughout the year*

*Fig. 9* and *Fig. 10* illustrate the profiles of load demand, PV generation, SoC of the Li-ion battery, and the hydrogen storage energy state for a summer day and the worst-case winter day, respectively.

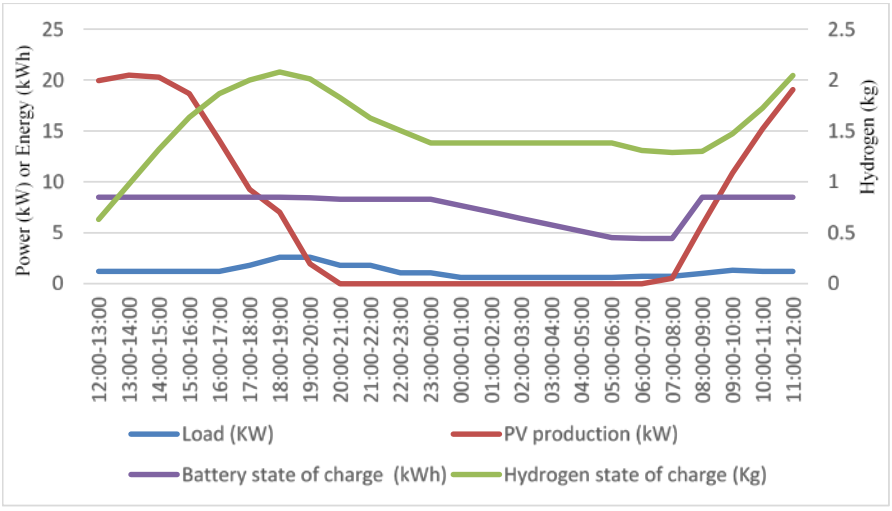


*Fig. 9. The load demand [kW], PV generation [kW], the energy state of the battery [kWh], and the energy state of the hydrogen storage tank [kg] on a summer day*

On a summer day (*Fig. 9*), PV generation is high during daylight hours (12:00–19:00). The surplus energy is initially used to charge the Li-ion battery until it reaches its maximum SoC. Once fully charged, any excess PV energy is directed

toward hydrogen production via the PEM electrolyzer, as indicated by the increasing state of energy in the hydrogen storage tank. In the evening (19:00–00:00), when PV generation ceases, the Li-ion battery supplies power for five minutes to compensate for the energy deficit, allowing the PEM fuel cell to warm up. Once the PEM fuel cell reaches operational capacity, it assumes the load, and the Li-ion battery ceases discharging. During the night (00:00–06:00), the fuel cell shuts down, and the Li-ion battery supplies power for the standby load. The following day, surplus PV energy is again prioritized for charging the Li-ion battery, with any remaining energy allocated to hydrogen production via the PEM electrolyzer.

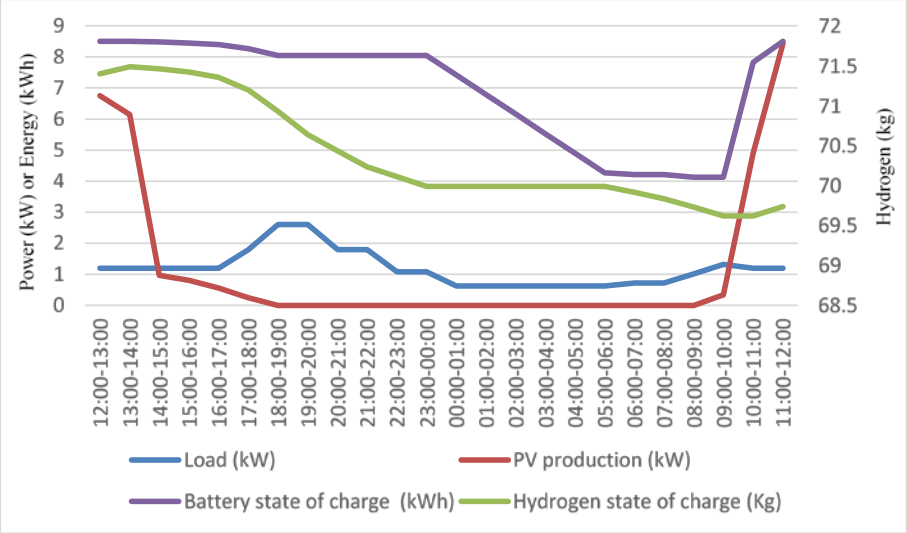


*Fig. 10. The load demand [kW], PV generation [kW], SoC of Li-ion battery [kWh], and the energy state of the hydrogen storage tank [kg] on a worst-case winter day*

On the worst-case winter day (Fig. 10), PV generation meets the demand only between 12:00 and 14:00. During the remaining hours, PV output is minimal, requiring the Li-ion battery to supply power for five minutes to compensate for the energy deficit while the fuel cell warms up. Once the fuel cell reaches full operational capacity, it assumes the load demand (14:00–00:00), and the Li-ion battery ceases power delivery. During nighttime hours (00:00–06:00), the PEM fuel cell shuts down, and the Li-ion battery supplies the standby load. The following day, as PV generation increases, surplus energy is first allocated to charging the Li-ion battery until it reaches its maximum SoC, ensuring immediate availability for short-term demand coverage and providing sufficient capacity to supply the next night's standby load. Once the Li-ion battery is fully charged, any additional PV energy is directed toward hydrogen production via the PEM electrolyzer.

The operational analysis verifies that all components of an off-grid PV-$H_2$-SS are appropriately sized to meet the required energy demands, ensuring an effective energy balance. Hydrogen is primarily produced during the summer for utilization during the winter, while the PV system generates sufficient electricity daily to charge the Li-ion battery, accommodate short-term energy demand coverage, and supply the nighttime standby load. By integrating Li-ion batteries for short-term and hydrogen storage for long-term stability, the PV-$H_2$-SS effectively manages energy resources, ensuring reliable and sustainable operation.

The Levelized Cost of Electricity (LCOE) represents the discounted cost per unit of electricity produced over the lifespan of a project. It serves as a fundamental metric for comparing different energy technologies, providing an objective assessment of their economical viability [19]. The economic feasibility of the proposed off-grid PV-$H_2$-SS is evaluated by analyzing its LCOE. The economic analysis of the off-grid PV-$H_2$-SS relies on cost parameters outlined in *Table 3*.

*Table 3*

*Cost parameters of the Off-Grid PV- H2-SS*

| Components | CapEx (1$=1€) | | OpEx % of CapEx ($/year) | References |
|---|---|---|---|---|
| | Investmen cost | Replacement cost, liftetime | | |
| PV modules | 234 *$/kW* | 25 years | 1 | [20,21] |
| BOS | 400 *$/kW* | 25 years | | |
| PEM Electrolyzer | 1400 *$/kW* | 400 *$/kW* Stacks replaced every 80,000 *h* or 10 years | 4 | [22,23] |
| PEM Fuel cell | 3000 *$/kW* | 1052 *$/kW* Stacks replaced every 10 years | 0.9 | [24-26] |
| Hydrogen storage | 470 *$/kg* | 30 years | 1.5 | [26,27] |
| Li-ion Battery | 237 *$/kWh* | 237 *$/kWh* Lifetime is taken 10 years. | 2.5 | [28,29] |
| Compressor 0.7 *kW* | 300$ *$kgH_2/day$* from *Fig.7* max. daily $H_2$ production is 36.37 $Nm^3$(3.27kg) | 25 years | 0.5 | [30] |

Using the cost parameters outlined in Table 3, the investment costs for individual components of the PV-$H_2$-SS were calculated. The initial investment cost was determined to be $143,121. The cost distribution among the components

accounts for around: PV (4.08%), BOS (7%), electrolyzer (22.5%), fuel cell (6.29%), hydrogen storage (57.8%), battery (1.65%), and compressor (0.68%).

The LCOE of the off-grid PV-$H_2$-SS ($LCOE_{PV\text{-}H2\text{-}SS}$), expressed in *$/kWh*, is calculated using the following equation [31]:

$$LCOE_{PV-H2-SS} = \frac{\sum_{y=0}^{n} \frac{(C_{\mathrm{PV-H2-SS},y} + O_{\mathrm{PV-H2-SS},y})}{(1+r)^y}}{\sum_{y=1}^{n} \frac{E_{demand,y}}{(1+r)^y}}, \quad (9)$$

where $C_{\mathrm{PV-H2-SS,y}}$ represents the capital expenditure costs (CapEx) of the PV-$H_2$-SS in year *y* (including initial investment costs and major replacements in later years), $O_{\mathrm{PV-H2-SS,y}}$ denotes the operating expenditure (OpEx) costs in year *y* (In year 0, OpEx is zero) , *n* is the total project duration (25 years), *r* - the discount rate (6.57% for Armenia [32]) and $E_{demand,y}$ represents the electricity demand in year *y* (based on the daily load profile established in the previous section).

To assess the practicality and feasibility of the off-grid PV-$H_2$-SS, the study also examines the LCOE of extending the electrical grid. A distribution grid can be deployed in any environment where physical conditions permit. A grid extension comprises several components, including distribution transformers, circuit breakers, and transmission lines. The technical and economic parameters of the grid extension are analyzed in detail below.

The primary distribution voltage at the selected case study site is 6 *kV*, with a frequency of 50 *Hz*. The hourly energy consumption of the end user at the site was detailed in the previous section, with an annual total consumption of 10,482.8 *kWh*. Given this consumption and a peak demand of 2.6 *kW* during the fiscal year, a transformer with a 10 *kVA* capacity is selected, as it meets the minimum standard for a 6 *kV* distribution voltage.

In compliance with Armenian distribution network regulations, which align with international and regional standards, steel-aluminum conductors with a cross-sectional area of 35 *mm²* are minimum for 6 *kV* overhead lines to ensure safety and reliability [33]. The overhead line's current capacity is 160 *A*, which is adequate for supplying the case study site, given the maximum load demand of only 2.6 *kW*.

From an economic perspective, the evaluation of grid extension is based on two key cost parameters: CapEx and OpEx. CapEx includes all investment costs associated with design, installation, acquisition, and transportation of infrastructure. OpEx covers operation and maintenance expenses, as well as costs related to failures and repairs.

The cost parameters for grid extension, which are critical for economic analysis, are presented in *Table 4*.

*Table 4*

*Grid extension cost parameters*

| Cost type | CapEx [1AMD=400 USD] | OpEx % of CapEx (yearly) [1AMD=400 USD], Lifetime | References |
|---|---|---|---|
| 6 *kV* Electrical distribution network extension (Includes: design and engineering services, construction and installation works, 35 *mm²* aluminum-conductor steel-reinforced overhead line and associated hardware, load break switches, and metering equipment.) | 27656 *$/km* | 8 % | [34] |
| Transformer 10 *kVA* | 7275 *$* | 5 % | [34] |

The LCOE of the grid extension ($LCOE_{grid}$) is calculated using the following equation [31,35]:

$$LCOE_{grid} = \frac{\sum_{y=0}^{n}\left(C_{grid,y}+O_{grid,y}+EC_y\right)(1+r)^{-y}}{\sum_{y=1}^{n} E_{demand,y}(1+r)^{-y}}, \quad (10)$$

where $C_{grid,y}$ represents the CapEx for grid extension in year *y* (including initial investment costs), $O_{grid,y}$ denotes the OpEx in year *y* (in year 0, OpEx is zero.), $EC_y$ represents the annual electricity consumption cost from the grid in year *y* (considering the electricity tariffs in Armenia and the proportion of nighttime and daytime energy consumption at the case study site, the weighted average cost of 1 *kWh* is calculated to be $0.1287 [36], assuming 1 USD = 400 AMD).

Both energy supply options are compared in terms of LCOE. Using the cost parameters from *Table 3* and applying *Eq. 9*, the $LCOE_{PV\text{-}H2\text{-}SS}$ is calculated to be 1.48 *$/kWh*. In fact, it is obvious that feeding the case study site from the grid up to a certain distance creates lower costs than PV-H2-SS. Therefore, the $LCOE_{grid}$ is calculated for various distances, starting from 1 *km*, using the cost parameters from *Table 4* and applying *Eq. (10)*. The analysis helps determine the break-even point at which the off-grid PV-$H_2$-SS becomes economically viable compared to grid extension. This break-even distance is calculated as 3 *km* where the $LCOE_{grid}$ is found to be 1.51 *$/kWh*. In other words, extending the grid by 3 *km* or more for the case study site is not cost-effective, making the off-grid PV-$H_2$-SS the only economically viable solution.

***Conclusion.*** The technical and economical analysis of the proposed off-grid PV-$H_2$-SS confirms its technical viability and economic competitiveness for decentralized power supply, as demonstrated through a detailed case study in Hankavan, Armenia. The integration of PV solar power, electrolyzer, fuel cell, hydrogen storage tank, compressor, and Li-ion batteries was meticulously sized to ensure a consistent, year-round electricity supply despite fluctuations in solar energy availability and demand patterns.

The PV system efficiently meets the daily energy requirements and effectively charges the Li-ion battery, which functions as a critical short-term energy buffer. This battery storage supports the daytime transition periods (PEM fuel cell warm-up intervals) and the standby nighttime loads. Hydrogen generation, primarily concentrated during summer when solar resources are abundant, provides a sustainable solution to seasonal energy deficits, particularly in winter, reinforcing long-term energy reliability.

From an economic perspective, the calculated LCOE for the PV-$H_2$-SS stands at 1.48 *$/kWh*, making it competitive when compared with an electrical grid extension alternative, which has an LCOE of 1.51 *$/kWh* at a break-even distance of 3 *km*. This finding emphasizes the economic feasibility of deploying PV-$H_2$-SS in case study site situated 3 km or farther from existing grid infrastructure, especially relevant for rural and remote areas where the construction of a new grid infrastructure presents significant investment challenges.

Moreover, the adaptability of the PV-$H_2$-SS ensure its scalability, making it particularly suitable for various rural electrification scenarios. This off-grid solar PV-$H_2$-SS not only addresses the economic constraints associated with extending traditional energy infrastructure but also aligns with global sustainability goals by offering a clean, renewable, and efficient alternative. Consequently, adopting PV-$H_2$-SS technology could significantly contribute to energy independence, environmental conservation, and sustainable development in remote and off-grid regions worldwide.

## References


1. IEA (2024), CO2 Emissions in 2023, IEA. – Paris, 2024. https://www.iea.org/reports/co2-emissions-in-2023
2. **Boodoo C.** The True Cost of Off-Grid Solar Power: Evaluating Solar Energy in a Dense Tropical Forest // European Journal of Energy Research. - Jun. 2024.-Vol.4, No.2.- P.17-27.
3. The state of charge predication of lithium-ion battery energy storage system using contrastive learning / **Y. Xiong, T. He, W. Zhu, Y. Liao, et al** // Sustainable Energy Technologies and Assessments.- 2024.-Vol.71.- P.103989. DOI: https://doi.org/10.1016/j.seta.2024.103989

4. **Kummer K., Imre AR.** Seasonal and Multi-Seasonal Energy Storage by Power-to-MethaneTechnology // Energies.-2021.-14(11). - P.3265.DOI: https://doi.org/10.3390/en14113265
5. Integration of battery and hydrogen energy storage systems with small-scale hydropower plants in off-grid local energy communities / **L. Jin, M. Rossi, A.M. Ferrario, et al** // Energy Conversion and Management.- 2023.- Vol.286.-P.117019. DOI: https://doi.org/10.1016/j.enconman.2023.117019.
6. **Martinez Alonso A., Costa D., Messagie M., Coosemans T.** Techno-economic assessment on hybrid energy storage systems comprising hydrogen and batteries: A case study in Belgium // International Journal of Hydrogen Energy.- 2024.- Vol.52, part A.- P.1124-1135. DOI: https://doi.org/10.1016/j.ijhydene.2023.06.282
7. **Banasiak D. Kienberger T.** A comparative analysis of the economic feasibility of reversible hydrogen systems based on time-resolved operation optimisation // Applied Energy.-2024.-Vol.371.-P.123639.DOI. https://doi.org/10.1016/j.apenergy.2024.123639
8. **Qasem, Naef A.A., Abdulrahman, Gubran A.Q.** A Recent Comprehensive Review of Fuel Cells: History, Types, and Applications // International Journal of Energy Research. – 2024. – Vol.2024, issue 1, Article ID 7271748. – P.36. DOI: https://doi.org/10.1155/2024/7271748.
9. **Dickert J., Schegner P.** Residential load models for network planning purposes // Modern Electric Power Systems. – Wroclaw, Poland, 2010. - P. 1-6.
10. **Fischer D., Surmann A., Biener W., Selinger-Lutz O.** From residential electric load profiles to flexibility profiles – A stochastic bottom-up approach // Energy and Buildings.-2020.- Vol.224.- P.110133. DOI: https://doi.org/10.1016/j.enbuild.2020.110133
11. **Avoyan R.H.** Development of an off-grid solar power plant integrated with a hydrogen storage system // Proc. of the RA NAS and NPUA. Ser. of tech. sc. – 2024.- Vol. LXXVII, No.3.- P. 308-314.
12. Solar Energy the physics and engineering of photovoltaic conversion, technologies and systems / **A. Smets, K. Jäger, O. Isabella, et al**. - UIT Cambridge, 2016.- 488 p.
13. **El-Shafie M.** Hydrogen production by water electrolysis technologies: A review // Results in Engineering.- 2023.- Vol.20.- P.101426.
14. **Bhogilla S., Pandoh A., Singh U.R.** Cogeneration system combining reversible PEM fuel cell, and metal hydride hydrogen storage enabling renewable energy storage: Thermodynamic performance assessment // International Journal of Hydrogen Energy.- 2023. - Vol.52, part D.- P.1147-1155. DOI: https://doi.org/10.1016/j.ijhydene.2023.08.028
15. Lithium-ion Battery Cost Analysis in PV-household Application / **M. Naumann, R.C. Karl, C.N. Truong, et al** // Energy Procedia.- 2015.- Vol.73.- P.37-47. DOI: https://doi.org/10.1016/j.egypro.2015.07.555
16. **Abd El-Aal A. M., Schmid, J., Bard J.** Modelling and Simulation of a Stand-Alone Hydrogen Photovoltaic Fuel Cell Hybrid System for Long-Term Operation // International Journal of Modelling and Simulation.-2006.-Vol.26, No.4.- P. 370-377. DOI: https://doi.org/10.1080/02286203.2006.11442390

17. **Züttel A.** Hydrogen storage methods // Naturwissenschaften.- 2004.-Vol.91.- P.157-172. DOI: https://doi.org/10.1007/s00114-004-0516-x
18. **Khan M.A., Young C., MacKinnon C., Layzell D.** The Techno-Economics of Hydrogen Compression // Transition Accelerator Technical Briefs.- 2021.-Vol.1, issue 1.- P.1-36.
19. **Kabeyi M.J.B., Olanrewaju O.A.** The levelized cost of energy and modifications for use in electricity generation planning // Energy Reports.- 2023.-Vol.9, Supplement 9.- P.495-534. DOI: https://doi.org/10.1016/j.egyr.2023.06.036.
20. **IRENA** (2024). Renewable power generation costs in 2023. - International Renewable Energy Agency. - Abu Dhabi, 2024.
21. **Rodríguez-Martinez Á., Rodríguez-Monroy C.** Economic Analysis and Modelling of Rooftop Photovoltaic Systems in Spain for Industrial Self-Consumption // Energies.- 2021.- Vol.14, No.2.- P.7307. DOI: https://doi.org/10.3390/en14217307
22. **IRENA (2020).** Green Hydrogen Cost Reduction: Scaling up Electrolysers to Meet the 1.5ºC Climate Goal. - International Renewable Energy Agency. - Abu Dhabi**,** 2020.
23. **KMPG (June 2022).** How to evaluate the cost of the green hydrogen business case?. https://assets.kpmg.com/content/dam/kpmg/be/pdf/2022/hydrogen-industry-1.pdf
24. **IEA (2015).** Technology Roadmap - Hydrogen and Fuel Cells, IEA. – Paris, 2015. https://www.iea.org/reports/technology-roadmap-hydrogen-and-fuel-cells
25. **Cigolotti V., Genovese M., Fragiacomo P.** Comprehensive Review on Fuel Cell Technology for Stationary Applications as Sustainable and Efficient Poly-Generation Energy Systems//Energies.-2021.-14(16).-P. 4963. DOI: https://doi.org/10.3390/en14164963
26. **Parra D., Valverde L., Pino F. J., Patel M. K.** A review on the role, cost and value of hydrogen energy systems for deep decarbonisation // Renewable and Sustainable Energy Reviews.- 2019.-Vol.101.-P.279-294.DOI: https://doi.org/10.1016/j.rser.2018.11.010.
27. **Chardonnet C., Giordano V., De Vos L., Bart F.** Study on Early Business Cases for H2 in Energy Storage and More Broadly Power to H2 Applications // FCH-JU: Brussels, Belgium, 2017.-P.1-222. https://hsweb.hs.uni-hamburg.de/projects/star-formation /hydrogen/P2H_Full_Study_FCHJU.pdf
28. **Komorowska A., Olczak P., Hanc E., Kamiński J.** An analysis of the competitiveness of hydrogen storage and Li-ion batteries based on price arbitrage in the day-ahead market // International Journal of Hydrogen Energy.- 2022.- Vol.47, issue 66.-P. 28556-28572. DOI: https://doi.org/10.1016/j.ijhydene.2022.06.160
29. **National Renewable Energy Laboratory**. Residential battery storage.- 2023: Available: https://atb.nrel.gov/electricity/2023/residential_battery_storage
30. **HyETHydrogen**. Costs of HCS100 Hydrogen Compressor Stack. 2022, https://hyethydrogen.com/products/
31. **Pagnini L., Bracco S., Delfino F., de-Simón-Martín M**. Levelized cost of electricity in renewable energy communities: Uncertainty propagation analysis // Applied Energy.- 2024.- Vol.366.-P.123278. DOI: https://doi.org/10.1016/j.apenergy.2024.123278

32. **Central Bank of Armenia**. (2025). Monetary Policy Instruments Interest Rates. https://www.cba.am/en/sitepages/fmompiinterestrates.aspx
33. **Правила устройства электроустановок** (ПУЭ). Глава 2.5 "Воздушные линии электропередачи напряжением выше 1 кВ", пункт 2.5.77, таблица 2.5.5. https://etp-perm.ru/el/pue/razdel-2.-kanalizacziya-elektroenergii/pue-glava-2.5.-vozdushnyie-linii-elektroperedachi-napryazheniem-vyishe-1-kv
34. **«ՓԱՈՒԵՐ ԷՆԵՐՋԻ» ՍՊԸ** – ի կողմից 18.03.2025 թվականին տրված Թիվ ՎԹ – 50 տեղեկանք, Վ. Թարջումանյան:
35. **United Nations Development Programme (UNDP)**. **Touche Tohmatsu**. Task 1: Brief report on the comparison of the costs of grid extension to the alternative of decentralized RE based mini-grid. - October 2021. P.1-24.
36. **«Հայաստանի էլեկտրական ցանցեր» ՓԲԸ-ի** կողմից սպառողներին վաճառվող էլեկտրական էներգիայի սակագներ: https://www.ena.am/Info.aspx?id=11&lang=1

*Received on 27.12.2024.*
*Accepted for publication 24.03.2025.*

## ՋՐԱԾՆԱՅԻՆ ԿՈՒՏԱԿԻՉ ՀԱՄԱԿԱՐԳԻՆ ՀԱՄԱԿՑՎԱԾ ԻՆՔՆԱՎԱՐ ԱՐԵՎԱՅԻՆ ԿԱՅԱՆԻ ՏԵԽՆԻԿԱՏՆՏԵՍԱԿԱՆ ՀԵՏԱԶՈՏՈՒՄԸ. ԴԻՏԱՐԿՎՈՂ ՕԲՅԵԿՏԸ՝ ՀԱՆՔԱՎԱՆ (ՀԱՅԱՍՏԱՆ)

**Ռ.Հ. Ավոյան**

Հայաստանի Հանքավան բնակավայրում ուսումնասիրվող տեղանքի համար, որպես ինքնավար էներգամատակարարման լուծում, առաջարկվում է ջրածնային կուտակիչ համակարգին համակցված արևային ֆոտովոլտային էլեկտրակայանի (ՋԿՀՀԱՖՎԷԿ) կիրառումը: Ուսումնասիրվող տարածքի համար կազմվել է էլեկտրական բեռնվածքի օրական սպառման գրաֆիկը, և գնահատվել են առկա էներգետիկ ռեսուրսները, որոնց հիման վրա իրականացվել է ՋԿՀՀԱՖՎԷԿ – ի հիմնական բաղադրիչների՝ արևային ֆոտովոլտային (ՖՎ) համակարգի, էլեկտրոլիզի սարքի, վառելիքային տարրի, լիթիում-իոնային մարտկոցի, ջրածնի կուտակիչ համակարգի և կոմպրեսորի հզորությունների ու չափսերի ընտրություն: ՋԿՀՀԱՖՎԷԿ – ի շահագործման բնութագրերը հետազոտվել են՝ տարվա ընթացքում էլեկտրաէներգիայի անխափան և հուսալի մատակարարումն ապահովելու նպատակով: Շահագործման հետազոտության արդյունքները հաստատում են, որ ՋԿՀՀԱՖՎԷԿ – ի բոլոր բաղադրիչները ճիշտ են ընտրված՝ պահանջվող հզորություններին համապատասխան, և ապահովում են էլեկտրաէներգիայի պահանջները: Ջրածնի արտադրությունը հիմնականում իրականացվում է ամռան ամիսներին՝ ձմռան շրջանում էներգամատակարարումն ապահովելու նպատակով, և օգտագործվում է ցերեկային ժամերին (06:00–00:00) էներգիայի դեֆիցիտը ծածկելու համար: Միևնույն ժամանակ, ֆոտովոլտային համակարգն ամեն օր արտադրում է բավարար քանակությամբ էլեկտրաէներգիա՝ լիթիում-իոնային մարտկոցի լիցքավորումն ապահովելու համար: Մարտկոցն օգտագործվում է որպես կարճաժամկետ էներգետիկ բուֆեր, որը 5 *րոպե* տևողությամբ

ծածկում է ցերեկային էլեկտրաէներգիայի դեֆիցիտը՝ թույլ տալով վառելիքային տարրի նախնական տաքացումը, ինչպես նաև ապահովում է գիշերային ժամերին (00:00–06:00) մշտական բեռի սպառումը: Կախված կարճաժամկետ և երկարաժամկետ պահանջներից՝ իրականացվում է էլեկտրաէներգիայի օպտիմալ բաշխում լիթիում-իոնային մարտկոցների և ջրածնային կուտակիչի միջև: Ինքնավար ՋԿՀՀԱՖՎԷԿ–ի տնտեսական նպատակահարմարությունը գնահատելու համար նրա էլեկտրաէներգիայի համաճարթեցված արժեքը (ԷՀԱ) համեմատվում է էլեկտրացանցի ընդլայնման ԷՀԱ – ի հետ: Դիտարկվող օբյեկտի համար ՋԿՀՀԱՖՎԷԿ-ի տնտեսապես նպատակահարմար սահմանային հեռավորությունը կազմում է 3 *կմ*: ՋԿՀՀԱՖՎԷԿ -ի համար հաշվարկված ԷՀԱ – ն կազմում է 1.48 *$/կՎտժ*, իսկ էլեկտրացանցը 3 *կմ* ընդլայնելու դեպքում նրա ԷՀԱ-ն կազմում է 1.51 *$/կՎտժ*: Ստացված արդյունքների հիման վրա ինքնավար ՋԿՀՀԱՖՎԷԿ – ը համարվում է տնտեսական առումով նպատակահարմար դիտարկվող օբյեկտի դեպքում, երբ այն գտնվում է էլեկտրացանցից 3 *կմ* կամ ավելի հեռավորության վրա՝ ապահովելով մաքուր և կայուն այլընտրանք ինքնավար էներգամատակարարման համար: Բացի այդ, ստացված արդյունքները վկայում են, որ ՋԿՀՀԱՖՎԷԿ – ն կարող է մասշտաբավորվել կամ հարմարեցվել գյուղական բնակավայրերում կիրառման համար, որոնք հեռու են կենտրոնացված էլեկտրական ցանցերից, որտեղ նոր էներգետիկ ենթակառուցվածքների կառուցումը կպահանջի զգալի ներդրումներ:

***Առանցքային բառեր.*** արևային ֆոտովոլտային համակարգ, ջրածնային կուտակիչ համակարգ, էլեկտրոլիզ, վառելիքային տարր, լիթիում-իոնային մարտկոց, կոմպրեսոր, էլեկտրաէներգիայի համաճարթեցված արժեք:

## ТЕХНИКО-ЭКОНОМИЧЕСКИЙ АНАЛИЗ АВТОНОМНОЙ СОЛНЕЧНОЙ ЭЛЕКТРОСТАНЦИИ С ИНТЕГРИРОВАННОЙ ВОДОРОДНОЙ СИСТЕМОЙ ХРАНЕНИЯ: КЕЙС-СТАДИ НА ПРИМЕРЕ АНКАВАНА, АРМЕНИЯ

**Р.О. Авоян**

В качестве автономного источника энергоснабжения для исследуемого объекта в Анкаване (Армения) предлагается солнечная фотоэлектрическая станция, интегрированная с системой водородного хранения (СФЭССВХ). Определены профиль нагрузки и доступные энергетические ресурсы для данного участка. На основе этих данных произведены расчет и подбор основных компонентов СФЭССВХ, включая фотоэлектрическую установку, электролизер, топливный элемент, литий-ионный аккумулятор, водородное хранилище и компрессор. Операционная эффективность СФЭССВХ анализируется для обеспечения надежного электроснабжения в течение всего года. Результаты анализа эксплуатационных характеристик системы подтверждают, что все ее компоненты подобраны в соответствии с требуемой мощностью и удовлетворяют требованиям энергетического баланса. Водород вырабатывается преимущественно в летний период для последующего использования зимой и применяется для компенсации дефицита электроэнергии в дневное время (с 06:00 до 00:00). При этом фотоэлектрическая

система ежедневно вырабатывает достаточное количество электроэнергии для зарядки литий-ионного аккумулятора. Путем интеграции литий-ионных аккумуляторов для краткосрочной стабилизации и водородного хранилища для долгосрочного управления энергоресурсами СФЭССВХ обеспечивает эффективное регулирование энергетического баланса в течение года. Для оценки экономической целесообразности СФЭССВХ рассчитывается нормированная стоимость электроэнергии (НСЭ), которая сравнивается с НСЭ, связанной с расширением электрических сетей. Определенное для рассматриваемого объекта расстояние безубыточности составляет 3 *км*. Расчетная НСЭ для СФЭССВХ составляет 1,48 $/*кВт·ч*, тогда как НСЭ для расширения электрической сети на 3 *км* составляет 1,51 $/*кВт·ч*. На основании проведенного анализа автономная СФЭССВХ является экономически целесообразной для установки на рассматриваемом объекте при удаленности от электрической сети на 3 *км* и более, обеспечивая экологически чистую и устойчивую альтернативу децентрализованному энергоснабжению. Кроме того, полученные результаты подтверждают возможность масштабирования и адаптации данной системы для применения в сельских и удаленных районах, не подключенных к централизованным энергосистемам, где строительство новой энергетической инфраструктуры потребует значительных капитальных вложений.

***Ключевые слова:*** солнечная фотоэлектрическая система, система водородного хранения, электролизер, топливный элемент, литий-ионный аккумулятор, компрессор, нормированная стоимость электроэнергии.